Mineral dust and elemental black carbon records from an Alpine ice core (Colle Gnifetti glacier) over the last millennium

Florian Thevenon,[1,2] Flavio S. Anselmetti,[3] Stefano M. Bernasconi,[1] and Margit Schwikowski[4]

Received 18 November 2008; revised 21 April 2009; accepted 1 June 2009; published 2 September 2009.

[1] Black carbon (BC) and mineral dust aerosols were analyzed in an ice core from the Colle Gnifetti glacier (Monte Rosa, Swiss-Italian Alps, 45°55′N, 7°52′E, 4455 m above sea level) using chemical and optical methods. The resulting time series obtained from this summer ice record indicate that BC transport was primarily constrained by regional anthropogenic activities, i.e., biomass and fossil fuel combustion. More precisely, the $\delta^{13}C$ composition of BC suggests that wood combustion was the main source of preindustrial atmospheric BC emissions (C3:C4 ratio of burnt biomass of 75:25). Despite relatively high BC emissions prior to 1570, biomass burning activity and especially C_4 grassland burning abruptly dropped between 1570 and 1750 (C3:C4 ratio of burnt biomass of 90:10), suggesting that agricultural practices strongly decreased in Europe during this cold period of the "Little Ice Age" (LIA). On the other hand, optical analysis revealed that the main source for atmospheric dust transport to the southern parts of the Alps during summer months was driven by large-scale atmospheric circulation control on the dust export from the northern Saharan desert. This southern aerosol source was probably associated with global-scale hydrologic changes, at least partially forced by variability in solar irradiance. In fact, periods of enhanced Saharan dust deposition in the ice core (around 1200–1300, 1430–1520, 1570–1690, 1780–1800, and after 1870) likely reflect drier winters in North Africa, stronger North Atlantic southwesterlies, and increased spring/summer precipitation in west-central Europe. These results, therefore, suggest that the climatic pejorations and the resulting socioeconomic crises, which occurred in Europe during periods of the LIA, could have been indirectly triggered by large-scale meridional advection of air masses and wetter summer climatic conditions.

Citation: Thevenon, F., F. S. Anselmetti, S. M. Bernasconi, and M. Schwikowski (2009), Mineral dust and elemental black carbon records from an Alpine ice core (Colle Gnifetti glacier) over the last millennium, *J. Geophys. Res.*, *114*, D17102, doi:10.1029/2008JD011490.

1. Introduction

[2] Ice cores studies carried out on the Greenland and Antarctic polar ice sheets have provided the most detailed and best preserved long-term record of atmospheric particulate aerosols emitted by natural and anthropogenic sources [*Chylek et al.*, 1995; *Ruth et al.*, 2003; *Delmonte et al.*, 2004]. However, these glaciochemical records are only representative of the poleward long-range transport pattern of aerosols. In contrast, middle- and low-latitude glaciers, which are located within the principal source areas of continental aerosol species, offer complementary ice core records for studying the regional impact of the aerosols emitted by natural and anthropogenic sources. In this respect, the European Alps, which are surrounded by highly populated and industrialized countries, contain a few high-elevation areas adequate for ice core studies. In particular, the Colle Gnifetti glacier saddle, located in the Monte Rosa Massif at the Swiss-Italian border has been glaciologically characterized and identified as suitable for the recovery of long-term records [*Oeschger et al.*, 1977; *Alean et al.*, 1983; *Haeberli et al.*, 1983; *Schotterer et al.*, 1985]. The Colle Gnifetti glacier is characterized by a ice thickness reaching 60 to 130 m in the central saddle area [*Lüthi and Funk*, 2000], and by a low net snow accumulation of about 33 cm water equivalent per year (weq) resulting from the preferential wind erosion of dry winter snow [*Döscher et al.*, 1995]. The site has been drilled in 1976, 1982, 1995, and 2003, and borehole experiments indicate that meltwater percolation is negligible below the surface [*Haeberli and Funk*, 1991]. Consequently, the Colle Gnifetti saddle satisfactory conserves the accumulation history of summer precipitation chemistry and climatic conditions over relatively long time period (i.e., a few hundred to thousand years).

[3] Previous Alpine ice cores studies demonstrate that the anthropogenic aerosol concentrations increased following the

[1]Geological Institute, ETH Zurich, Zurich, Switzerland.
[2]Now at F.-A. Forel Institute, University of Geneva, Versoix, Switzerland.
[3]Eawag, Swiss Federal Institute of Aquatic Science and Technology, Dübendorf, Switzerland.
[4]Paul Scherrer Institut, Villigen, Switzerland.

0148-0227/09/2008JD011490

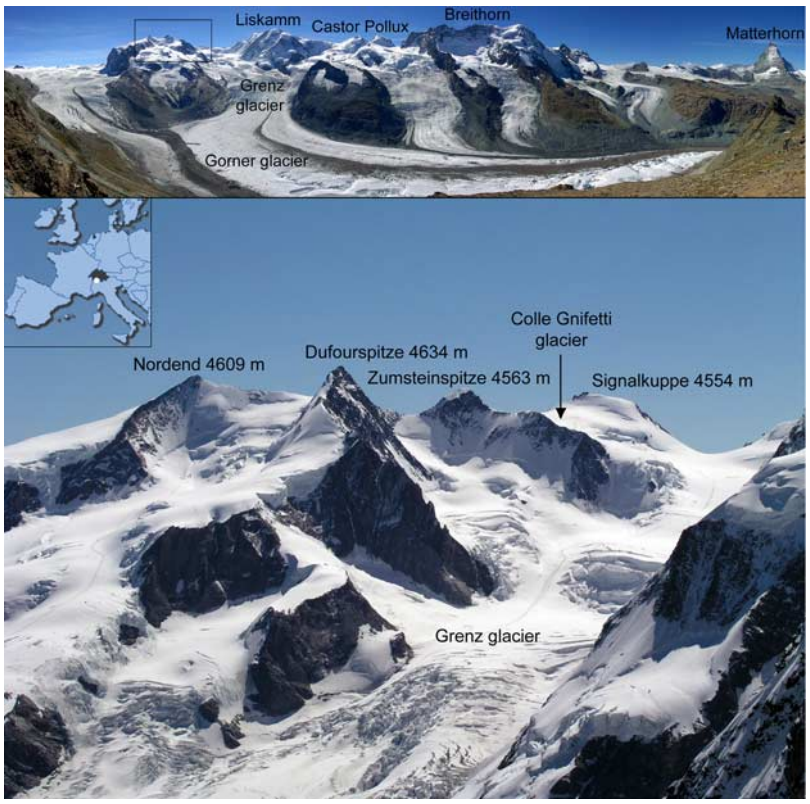

Figure 1. (top) Panorama from the south of the Monte Rosa Massif showing (from left to right) the Monte Rosa (square outline), Liskamm, Castor and Pollux (or Zwillinge), Breithorn, Matterhorn (or Cervin), and the Grenz and Gorner glacier (panorama photography by U. Raz). (bottom) The location of the studied area in Europe (left insert) and a view of the Monte Rosa showing (from left to right) Nordend, Dufourspitze, Zumsteinspitze, the Colle Gnifetti glacier, and Signalkuppe (or Punta Gnifetti; photography by F. Hunger).

onset of industrialization, and that these species are mostly deposited in summer, when polluted air is transported to high altitudes by convection [*Maupetit et al.*, 1995; *Lavanchy et al.*, 1999; *Eichler et al.*, 2004]. Whereas other Alpine ice records cover rather short time periods (i.e., few decades to hundred years), the Colle Gnifetti summer ice archive offers a unique possibility for reconstructing regional (pre)industrial carbonaceous aerosol emissions related to anthropogenic activities. Moreover, because of its orographic position in the Southern Alpine chain, the Colle Gnifetti glacier is strongly influenced by air masses advected from southerly directions [*Wagenbach and Geis*, 1989]. More precisely, the Southern Alps act as a barrier to the meridional transport of the southwesterly dust-laden winds from the Sahara during the spring/summer seasons, and Saharan dust is deposited on Alpine glaciers when coinciding with snowfall [*Sodemann et al.*, 2006]. The Colle Gnifetti summer archive therefore provides a valuable ice record for reconstructing changes in the dynamic of the southwesterly dust-laden winds from the Sahara, in relation to variability in large-scale atmospheric circulation.

2. Study Site and Ice Core Stratigraphy

[4] In 2003, a 80 m long ice core (corresponding to 62 m weq, CG03) was drilled to bedrock on the Colle Gnifetti glacier saddle (45°55′50″N, 7°52′33″E), located in the Monte Rosa Massif at an altitude of 4455 m above sea level (asl), near the Swiss-Italian border (Figure 1). Because of preferential wind erosion of light winter snow at this site, the glacier saddle accumulates snow mainly during summer and mean annual snow accumulation is only 0.454 ± 0.033 cm weq, implying preservation of more than the last 1000 years at a reasonable temporal resolution and, furthermore, the presence of more than 10,000 year old ice near the bedrock [*Jenk et al.*, 2009]. The dating of the ice core was performed by counting annual peaks of ammonium and by using stratigraphic horizons that are (1) the 1963 tritium horizon produced by the thermonuclear tests; (2) four visible yellowish dust horizons attributed to Saharan dust events of 1977, 1947, 1936, and 1901; and (3) two volcanic layers (Katmai 1912 and Laki 1783/1784). Radiocarbon dating and a glacier flow model were further used to establish the chronology (see details given by *Jenk et al.* [2009]). The resulting age-depth model indicates important layer thinning toward the bottom of the core, especially before the first millennium AD. Because the dating procedures required large amounts of ice in some sections, some samples could not be analyzed for particulate aerosols, resulting in two gaps in the record around 1300–1430 and 1960–1965, respectively.

3. Methods

[5] Samples from the ice core were prepared in the −20°C refrigerated room at the Paul Scherrer Institute

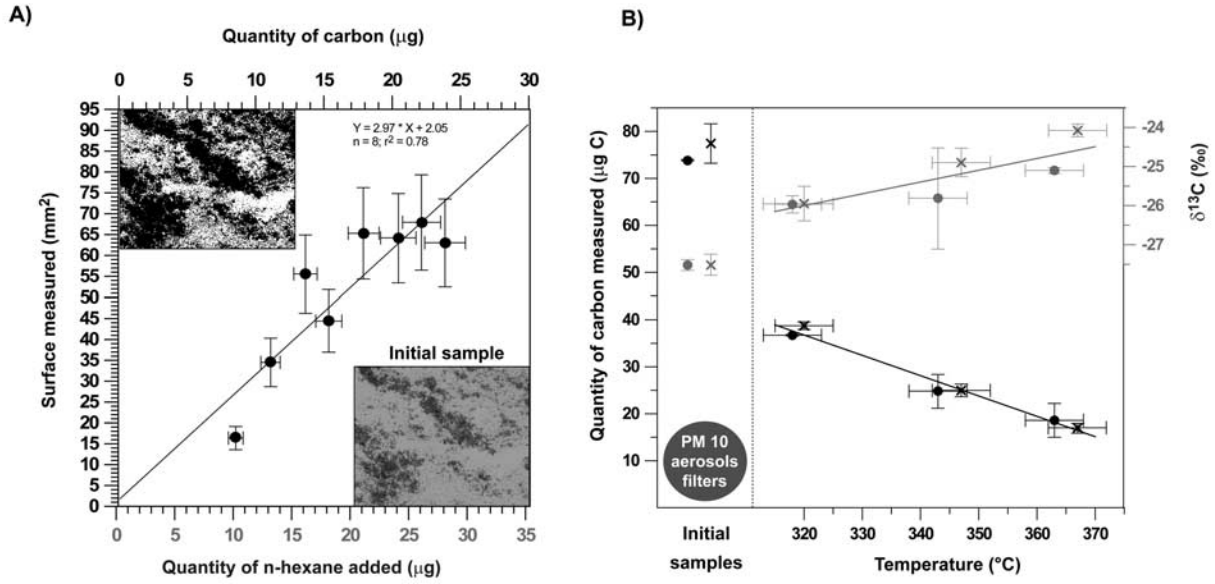

Figure 2. Calibration of the analytical procedures. (a) The optical image analysis technique detected the black surface (upper left) remaining after thresholding the gray level of the original image (bottom right), as a function of the quantity of carbon present on the microscope slide (and the corresponding initial quantity of *n*-hexane soot added). (b) The effect of the thermal treatment on two PM_{10} modern aerosol samples (cross and point) in black and the corresponding $\delta^{13}C$ composition in gray. The initial values of the samples are shown to the left of the dotted line, attesting that half of the original carbon was removed at the selected temperature of 320 ± 5°C.

(PSI) Villigen, Switzerland. Prior to sampling, visual stratigraphy was described and density was measured on core sections (about 60 cm long). Cutting of the ice core sections and removal of possibly contaminated outer layers were performed using a precleaned stainless steel band saw. The outermost part of the core was used for the optical analysis, while the inner part, which was contaminant free, was used for the elemental carbon analysis. Afterward, the frozen samples (0.2 up to 0.9 kg) were rinsed with ultrapure water (Millipore, Milli-Q, 18MΩ; mass loss 10 to 20%) to remove possible surface contamination by dust and fibers from clothes. Subsequently, the samples were weighted and stored in precleaned polyethylene containers and melted at room temperature before being filtered.

3.1. Total and Mineral Aerosols Image Analysis

[6] Aerosol surface and grain size were determined by image analysis. For this purpose, the melted ice was passed through a mixed cellulose ester membrane filter (47 mm diameter, 0.22 μm pore size; Advantec MFS, Inc.). These filters were then mounted onto a microscope smear slide for observation through an automated transmitted light microscope equipped with a black and white scan camera connected to a video frame grabber (images of 1600 × 1200 pixels, pixel size is 0.16 μm). Total and mineral (i.e., true crystalline material) aerosols were isolated from the background of the images acquired with transmitted white light and plane-polarized light, respectively. The particles having a different gray-level value from the background were extracted after thresholding the gray level of the grabbed images (Figure 2a) using Image/J software (Rasband, WS, Image J, NIH, Bethesda, MD, USA). The abundance of amorphous and opaque minerals as well as the presence of the organic phase may have resulted in an underestimation of the absolute mineral fraction. However, independent optical observations indicated that that the minerals isolated by this procedure were mostly quartz particles, which are predominant in Saharan dust emissions [*Adedokun et al.*, 1989; *Goudie and Middleton*, 2001; *Moreno et al.*, 2006]. Although a minor contribution by other quartz sources cannot be excluded (e.g., wind erosion on agricultural soils, industrial fly ash particles), our results showed that this method provides a valuable proxy for Saharan dust emissions (see section 4.1).

[7] This optical procedure, previously developed for studying microcharcoal from sedimentary archives [*Thevenon et al.*, 2003], was calibrated using a soot reference material (*n*-hexane, 0.853 gC/g, standard deviation SD = 0.038, n = 5). The surface remaining after subtracting the background of the images was computed and expressed as a function of the quantity of carbon added (Figure 2a; Y = 2.970 X + 2.056). However, the relationship between the surface measured and the quantity of added carbon from *n*-hexane has a moderate correlation coefficient (r^2 = 0.78) because the particles tend to aggregate and because of heterogeneities on the smear slides.

[8] Further analyses on individual mineral dust particles were performed using Scanning Electron Microscopy with Energy Dispersive X-ray Spectrometer (SEM/EDX) and Laser Ablation Inductively Coupled Mass Spectrometry (LA-ICP-MS). Backscatter images (BSE) were acquired using a FEI Quanta 200F field emission SEM (of the Electron Microscopy ETH Zurich, EMEZ) operated at 10 kV and in low vacuum (~50 Pa) mode. LA-ICP-MS analyses were performed using a prototype homogenized 193 nm Argon fluorine laser ablation system in combination with a quadrupole ICP-MS (PerkinElmer Elan 6100 DRC of the Institute of

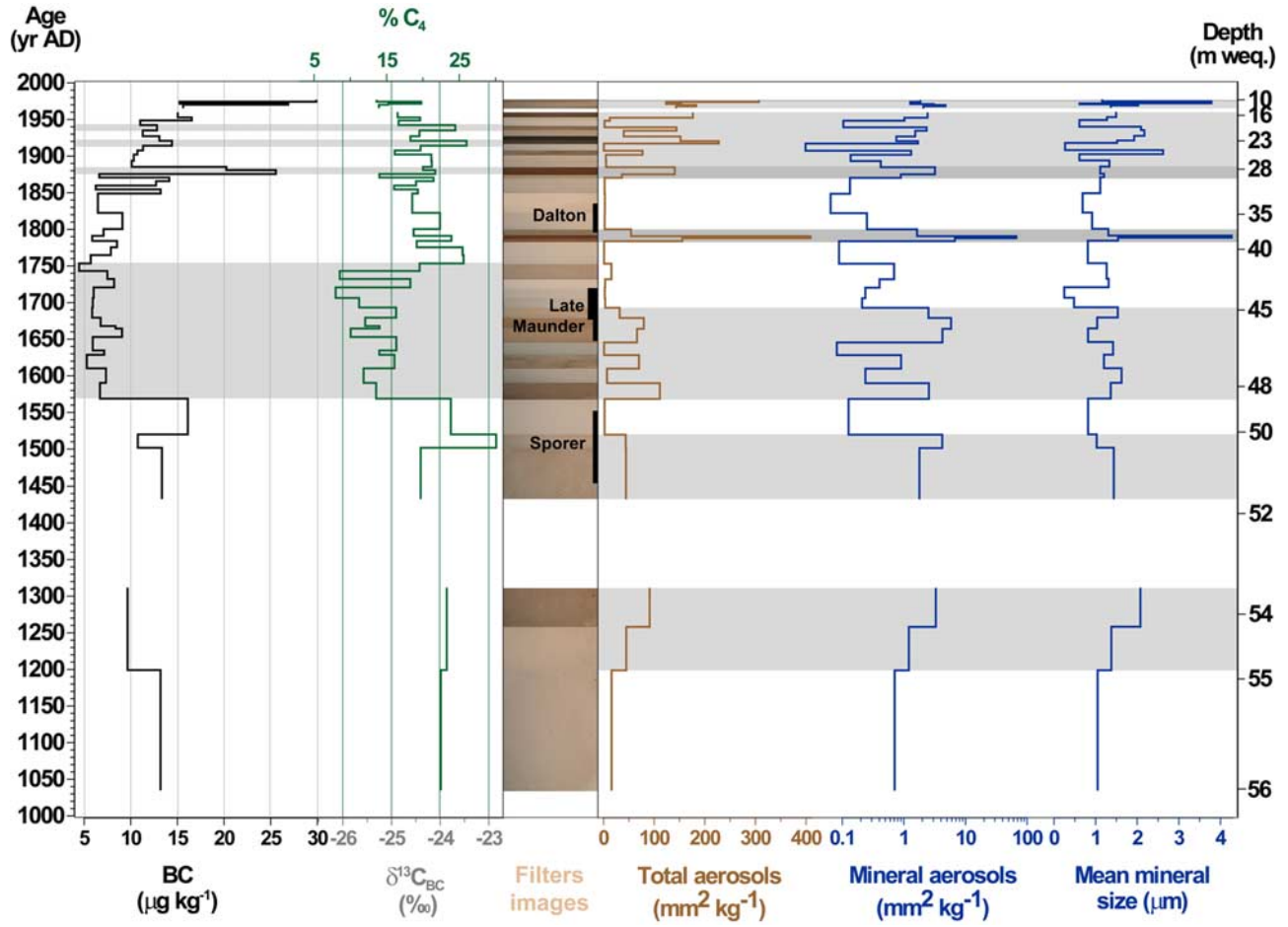

Figure 3. The last millennium record of black carbon (BC) concentration and the associated $\delta^{13}C_{BC}$ composition, as a function of age (year A.D.; left axis) and depth (meter water equivalent (m weq); right axis). The digital images of the filters, the total and mineral (crystalline) aerosol records, and the mean diameter of the mineral fraction are shown. The three last major solar anomalous periods, the Spörer, the (Late) Maunder, and the Dalton Minima, are reported for comparison. The gray shaded areas are discussed in the text.

Isotope Geochemistry and Mineral Resources ETH Zürich). Helium was used as carrier gas and NIST SRM 610 glass as standard reference material.

3.2. Black Carbon Elemental Analysis

[9] The samples for the elemental black carbon (BC) analysis were filtered through preheated (12 h at 1000°C) quartz fiber filters (Pallflex 2500 QAT-UP; 0.3 μm pore size). Microgram-level carbon concentration and isotopic composition were determined simultaneously with a CE instrument NCS 2500 elemental analyzer coupled to a Micromass OPTIMA mass spectrometer; after removing carbonates by HCl acidification (i.e., by pipetting 100 μL of 1M HCl 3 times onto the sample spot) and organic carbon compounds (i.e., thermal oxidation of organic matter). The thermal technique relies on heating of samples in the presence of oxygen, in order to remove organic carbon, which is volatilized or oxidized leaving BC in the sample [*Cachier et al.*, 1989]. The filters were then placed into pressed tin pans (4.25 × 12.5 mm ultralight weight and precleaned; Elemental Microanalysis) and folded with forceps. The sample and the tin container were oxidized to CO_2 in an oxygen-enriched atmosphere. Combustion of the sample occurred at temperature >1200°C, thus providing combustion of refractory carbonaceous material. Carbon isotope values are reported in the conventional delta notation relative to the Vienna-Pee Dee Belemnite (V-PDB) standard.

[10] The elemental analyzer was calibrated for carbon measurement by least squares linear regression with a soil reference sample (HEKAtech) containing 0.14% C, allowing to weight small masses of carbon (<10 μg). Additional atropine standard (HEKAtech) containing 70.56% C was used for the carbon isotopic calibration ($\delta^{13}C = -23.83‰$; n = 6; SD = 0.07). Blanks were determined by cutting and analyzing artificial ice, prepared by freezing of ultrapure water. Filter blanks were determined by filtering around 0.5 kg of this prepared artificial ice, and were equivalent to 0.32 μg C (n = 4; SD = 0.16). The detection limit of the apparatus was defined as 3 times the SD of the filter blank loads (0.48 μg C), and the limit of quantification was defined as 10 times the SD of the filter blank loads (1.64 μg C). Because the Colle Gnifetti ice core contained relatively small amounts of BC (from 5 to 30 μg kg^{-1}), a continuous

Table 1. Laser Ablation ICP-MS Results

		Quartz Grain (n = 7)		Micas (n = 3)		Amphibole (n = 3)		
LA-ICP-MS	Unit	Mean	SD	Mean	SD	Mean	SD	Aggregate (n = 1)
SiO_2	wt %	88.22	2.84	45.25	1.22	59.32	1.80	30.17
TiO_2	wt %	0.08	0.02	0.14	0.02	0.03	0.02	0.19
Al_2O_3	wt %	0.84	0.32	32.75	2.48	15.37	3.70	6.22
FeO	wt %	0.32	0.12	4.65	0.60	4.45	1.28	5.27
MnO	wt %	0.01	0.01	0.39	0.33	0.03	0.02	0.35
MgO	wt %	0.31	0.14	2.06	0.17	5.47	7.41	0.65
CaO	wt %	1.03	0.29	0.05	0.03	4.02	0.96	47.20
Na_2O	wt %	5.16	1.25	0.70	0.27	9.60	2.24	0.10
K_2O	wt %	0.33	0.04	9.03	0.89	0.07	0.02	2.71
Li	ug/g	17.65	8.00	193.92	35.54	2.00	0.25	32.00
Sc	ug/g	18.59	4.89	9.28	0.97	15.94	1.82	28.21
V	ug/g	16.93	3.56	145.34	12.82	114.57	34.05	88.47
Cr	ug/g	255.90	36.90	30.40	4.39	230.43	25.01	58.80
Co	ug/g	4.60	2.24	323.26	65.44	25.43	2.67	8.99
Ni	ug/g	139.41	54.15	641.34	146.72	160.72	10.96	49.38
Cu	ug/g	439.69	137.10	228.91	32.75	13.09	3.52	4.72
Zn	ug/g	336.39	55.75	240.80	75.22	65.19	20.73	58.05
Rb	ug/g	13.21	3.39	414.57	23.07	0.34	0.13	154.57
Sr	ug/g	29.26	7.81	106.41	30.91	35.28	5.70	702.91
Y	ug/g	2.88	1.08	1.53	0.14	2.72	0.45	13.14
Zr	ug/g	26.64	9.70	0.69	0.10	0.87	0.10	0.52
Nb	ug/g	3.01	1.02	1.27	0.46	0.12	0.03	6.44
Sm	ug/g	4.63	1.49	0.29	0.05	0.66	0.24	0.64
Cs	ug/g	1.20	0.29	16.79	1.94	0.06	0.03	5.51
Ba	ug/g	26.21	4.26	1180.89	134.56	2.62	0.42	200.87
La	ug/g	2.74	0.50	0.10	0.02	0.13	0.06	4.55
Ce	ug/g	1.76	0.21	0.93	0.17	0.44	0.10	7.10
Pr	ug/g	1.38	0.73	0.06	0.03	0.07	0.02	0.66
Nd	ug/g	4.29	1.17	0.33	0.04	0.68	0.15	4.05
Eu	ug/g	1.78	0.46	0.21	0.12	0.18	0.05	0.23
Gd	ug/g	6.29	1.65	0.64	0.12	0.64	0.12	1.39
Tb	ug/g	0.73	0.22	0.06	0.02	0.09	0.03	0.11
Dy	ug/g	3.14	1.01	0.52	0.16	0.42	0.16	1.17
Ho	ug/g	1.35	0.39	0.07	0.02	0.09	0.02	0.29
Er	ug/g	4.63	1.06	0.20	0.04	0.30	0.04	1.16
Tm	ug/g	0.83	0.22			0.05	0.01	0.27
Yb	ug/g	6.25	0.38	0.25	0.04	0.37	0.13	2.32
Lu	ug/g	0.76	0.11			0.06	0.01	0.35
Hf	ug/g	5.24	1.49	0.15	0.02	0.46	0.07	0.11
Ta	ug/g	0.90	0.16			0.05	0.02	0.20
Pb	ug/g	16.33	2.11	41.64	7.63	0.38	0.10	15.35
Th	ug/g	3.49	0.57			0.05	0.01	1.54
U	ug/g	0.83	0.22	0.61	0.07	0.05	0.03	0.11

measurement of carbonaceous aerosols was performed by merging 2 to 4 ice section samples (0.2–0.9 kg of ice).

[11] The thermochemical treatment was calibrated (Figure 2b) using PM_{10} (particulate matter <10 μm in aerodynamic diameter) ambient aerosol samples collected at a roadside location in the city of Bern, a station from the Swiss National Monitoring Network for Air Pollution (NABEL). The results showed that a lowering of the oxidation temperature from 365, to 345 and to 320 ± 5°C detected about 24, 33, and 50% of the original carbon content, respectively (Figure 2b). The thermal treatment at 320°C was selected for removing the organic material and to facilitate the data comparison with previous studies from the Colle Gnifetti glacier [*Lavanchy et al.*, 1999] and from the Fiescherhorn glacier [*Jenk et al.*, 2006], in which the average loss of carbon was estimated as 50% for similar modern aerosol samples (S. Szidat, personal communication, 2006). The detail of this heating procedure was the following: Samples were placed in room temperature oven, which was heated with 5°C/min to 270°C, and then a second ramp of 1°C/min to reach 300°C, and finally a third ramp of 1°C/min to reach 320°C. Each of these heating steps was separated by 10 min for stabilizing the temperature, and the thermal oxidation at 320°C lasted 15 min. As observed in Figure 2b, the $\delta^{13}C$ value of the refractory carbon fraction increased with the temperature of oxidation, suggesting the removal of remnant organic material not completely oxidized during the combustion process. This thermochemical treatment was finally calibrated upon the carbonaceous particle reference material NIST urban dust SRM 1649a (0.179 gC/g, SD = 0.009, n = 5), showing that about 57% of the carbon was removed at 320°C (0.077 gC/g, SD = 0.003, n = 5). However, this value may be slightly underestimated, because the oxidation was interrupted 30 min after the end of the heating procedure, whereas for the other samples, the furnace was allowed to reach room temperature.

4. Results and Discussion

4.1. Saharan Dust Aerosols

[12] The insoluble particles from the Colle Gnifetti ice core reveal a brown-reddish color (Figure 3), typical of the

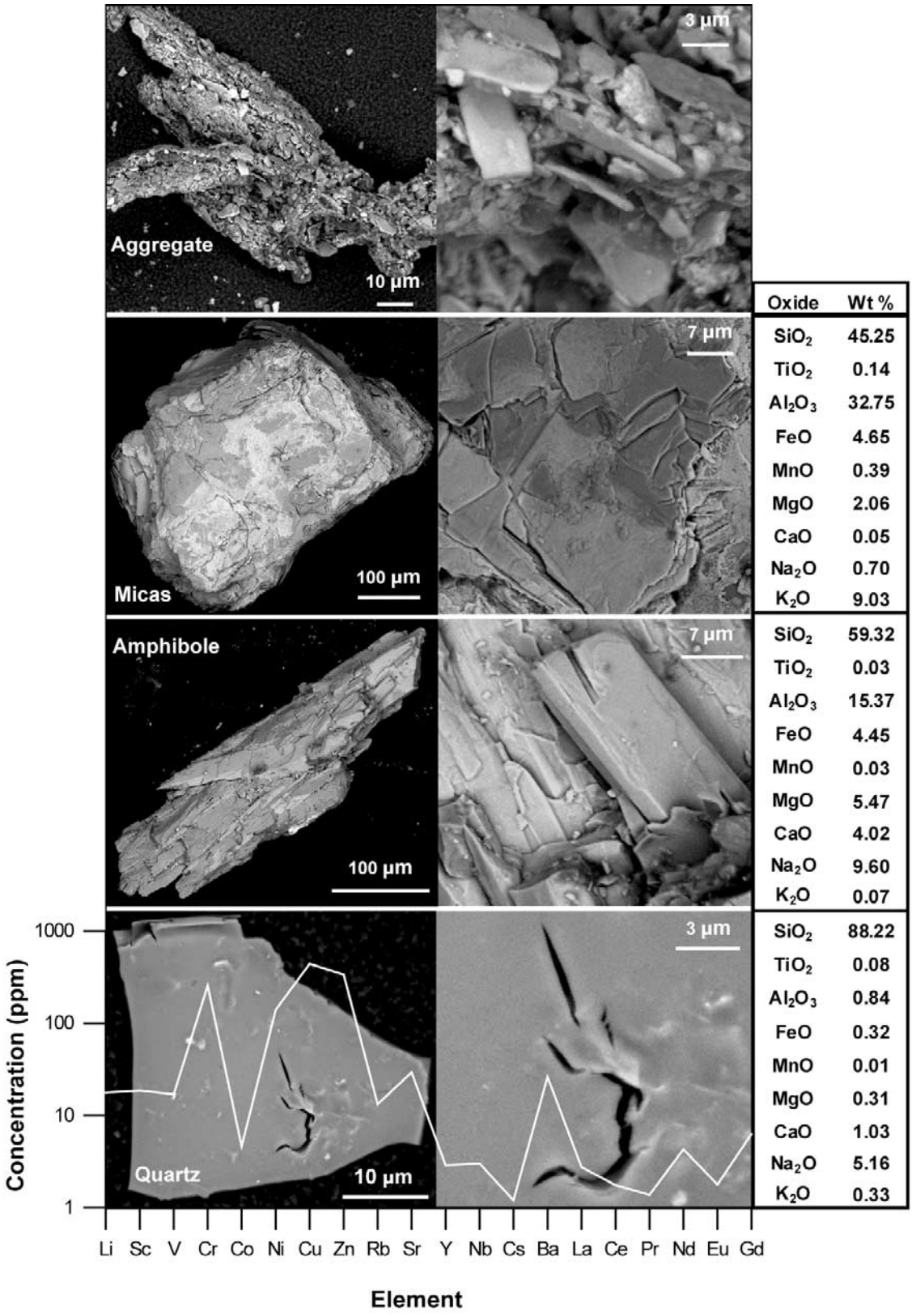

Figure 4. Scanning electron images of mineral particles from the Colle Gnifetti glacier ice core. Average major (wt % oxides) composition of three individual mineral particles determined by Laser Ablation Inductively Coupled Mass Spectrometry (LA ICP-MS), and the trace (ppm) element composition of the quartz particles from the largest Sahara dust event (approximately 1780–1800).

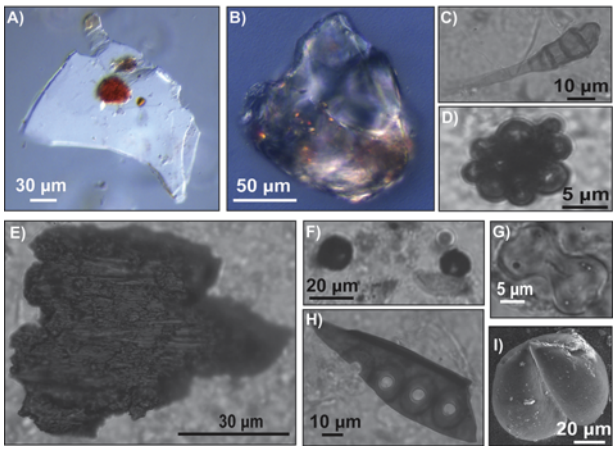

Figure 5. Transmitted-light microscope images from the Colle Gnifetti glacier ice core showing (a) a small and reddish rounded particle on a thin quartz fragment with a sharp and angular shape from the largest Sahara dust event (approximately 1790), (b) a thick subangular quartz particle, (c) a spore of fungi, (d) a green algae, (e) a large charcoal particle, (f) two fly ash particles from fossil fuel combustion, (g) a phytolith, (h) a piece of wood, and (i) a scanning electron image of a pollen grain.

Saharan dust events [*Krueger et al.*, 2004]. Moreover, the crystalline mineral record exhibits the same pattern of variations as the total aerosol record (Figure 3), suggesting Saharan dust as major component of total aerosol mass. Indeed, the mean diameter of the minerals within the largest dust outbreaks preserved in the Colle Gnifetti ice core range between approximately 2 and 4 μm (mean of 1.31 μm over the entire record), which matches variations in Saharan dust particle size transported to the Colle Gnifetti site over the last decades [*Wagenbach and Geis*, 1989; *Schwikowski et al.*, 1995]. On a longer timescale, these results from the Colle Gnifetti ice core are therefore in agreement with the contemporaneous dust transport to the Alps, strongly controlled by the southwesterly dust-laden winds from the northern and northwestern part of the Saharan desert [*Collaud Coen et al.*, 2004].

[13] The largest feature in the dust record of the last millennium is observed between approximately 1780 and 1800. The quantity of dust deposited during this time period is almost equivalent to the amount of dust deposited from the beginning of the record to the industrial revolution (approximately 1000–1850). This outstanding Saharan dust event might therefore be used as a reference horizon for dating other European ice and sediment records, which lack other appropriate dating tools for this period. That is the reason why additional geochemical analyses were performed on individual mineral particles from this large-scale environmental event: SEM/EDX and LA-ICP-MS (Table 1) analyses reveal abundant thin quartz fragments with a sharp and angular shape and a SiO_2 content over 85 wt %, containing the following trace elements: Cu (440 ppm), Zn (336 ppm), Cr (256 ppm), Ni (139 ppm), Sr (30 ppm), Zr and Ba (26 ppm), Li (18 ppm), Pb (16 ppm), and Rb (13 ppm) (Figures 4 and 5a). Some giant (>100 μm) and thick subangular quartz particles (Figure 5b) and monomineralic or agglomerates of silicate grains are also present throughout the ice core (Figure 4). However, the rare giant lithogenic particles are observed in layers depleted in aerosols, and geochemical analysis reveal that these minerals are not characteristic of the long-range soil-derived aerosols from the Sahara, but may rather represent a minor contribution of local sources, such as the Alpine gneiss making up the Monte Rosa Massif (e.g., micas, amphibole; Figure 4). Therefore, our results are in agreement with former studies on the Colle Gnifetti site, showing that the mineral background aerosol is very low (about 1 $\mu g\ m^{-3}$ in summer), and that the bulk impurity content of the glacier is largely dominated by Saharan mineral dust [*Haeberli et al.*, 1983; *Schotterer et al.*, 1985; *Wagenbach et al.*, 1985].

[14] Today, Saharan dust transport to the Alps is strongly influenced by the changes in winter precipitation over northern Africa and by the spring/summer pressure gradient in the North Atlantic [*Prospero and Nees*, 1986; *Chiapello and Moulin*, 2002]. During periods with high North Atlantic Oscillation (NAO; an index of air pressure difference between Iceland and the Azores/Iberia) conditions, the deepening of the Icelandic low pressure associated with a stronger Azores anticyclone induces a northward shift of the North Atlantic westerlies. This leads to drier conditions over the Mediterranean and northern Africa. Such drought conditions over North Africa enhance the dust mobilization over the Saharan desert and its transport over the Mediterranean Sea through southwesterly winds [*Middleton*, 1985; *Moulin et al.*, 1997]. That is the reason why the periods of enhanced Saharan dust deposition that occurred around 1200–1300, 1430–1520, 1570–1690, 1780–1800, and after 1870 (the gray shaded areas on Figure 3) may coincide with periods of stronger North Atlantic southwesterlies, drier winters over North Africa and wetter spring/summers over western-central Europe. In contrast, the periods of low Saharan dust mobilization and meridional transport to the Southern Alps in between those periods (approximately 1000–1200, 1520–1570, 1690–1780 and 1800–1870; Figure 3) may correspond to periods with weaker North Atlantic southwesterlies which are at present a source of warmth and moisture to Europe. Although such climatic features may be at least partially associated to the past NAO-like patterns of variability, the NAO versus Saharan dust relation is difficult to establish, considering that (1) the Alps are situated in a band of varying NAO influence [*Casty et al.*, 2005], (2) the influences of the NAO can change over time and region [*Jones et al.*, 2003], and (3) that there is no agreement among the reconstructions about the state of the NAO in the preindustrial era [*Schmutz et al.*, 2000; *Luterbacher et al.*, 2002]. However, there is supporting evidence for a connection between Saharan dust export to the Alps and changes in NAO, based on widespread evidence for increased negative states of the NAO during late 17th and early 18th century, probably as a large-scale dynamical response of the atmosphere to the estimated decrease in solar irradiance during the Late Maunder Minimum (1675–1715; Figure 3) [*Shindell et al.*, 2001]. The solar variability had an important influence on the global climate on decadal to centennial timescales, and at least three major solar anomalous periods can be identified in the climate of the past 500 years that are the Spörer (1450–1550), the Maunder (1645–1715), and the Dalton Minima

(1785–1830; Figure 3) [*Lean and Rind*, 1999]. The Saharan dust deposition was relatively low during the latter parts of these solar minima (Figure 3), suggesting a major solar influence in summer atmospheric circulation patterns, probably coupled with North Atlantic surface ocean temperature changes [*Dawson et al.*, 2007]. Furthermore, the 19th century was characterized by reduced solar irradiance when compared to the strong increase in solar activity during the first half of the 20th century. In fact, this latter increase coincides with more positive NAO indices and meridional atmospheric patterns [*Intergovernmental Panel on Climate Change*, 2007] as well as higher Saharan dust influx the ice record (Figure 3).

[15] Besides the solar forcing and anthropogenic influences (land use changes, greenhouse gases and industrial aerosol emissions), explosive volcanism represents the dominant external forcing of climate variability on timescales of the past two millennia [*Mann*, 2007]. Hence, important pulses of explosive volcanism during the Dalton Minima (e.g., Laki 1783/1784 and Tambora 1815) may have significantly contributed to the climate variability and cooling during this part of the "Little Ice Age" (LIA, approximately 1200–1850 [*Grove*, 1987; *Crowley*, 2000]). Although the apparent age (calculated by the age model) locates the highest concentration of Saharan dust between 1785 and 1790 (39.62 and 39.10 m weq), this horizon stratigraphically precedes the reference horizon of the Laki fissure eruption (apparent age of 1795, 38.81 m weq [*Jenk et al.*, 2009]), which began on June 1783 in Iceland. Therefore, the largest Saharan dust event just preceded the European climatic response to the intense sulphur gas emission of the Laki eruption, so that the dust increase cannot be related to this effect of explosive volcanism. We rather interpret the abrupt strengthening of the North Atlantic southwesterlies that occurred in the late eighteen century, as at least partial response to the relatively high solar activity that prevailed at that time rather than to explosive volcanic activity [*Metrich et al.*, 1991; *Crowley*, 2000; *Highwood and Stevenson*, 2003].

[16] Two of the largest Saharan dust events deposited in the Southern Alps over the last millennium around 1790 and 1880 (Figure 3) strikingly correspond with the two largest increases in atmospheric dustiness as recorded from high Himalayan ice cores over the same time period, around 1785 and 1875, respectively [*Thompson et al.*, 2000]. These Himalayan events coincide with two major failures of the South Asian monsoon, which resulted in devastating Indian droughts that suggest, along with other evidence, a relation between the Asian monsoon dynamics and the El Niño-Southern Oscillation (ENSO) variability [*Charles et al.*, 1997; *Cole et al.*, 2000; *Thevenon et al.*, 2004]. The identification of great Saharan events in the Alpine ice core that are roughly synchronous with low-latitude atmospheric circulation changes, may thereby support a large-scale atmospheric teleconnection pattern linking the North Atlantic trade winds circulation to the Intertropical Convergence Zone (ITCZ), probably coupled with meridional atmosphere and ocean heat transports/exchanges on interannual to decadal timescales [*Black et al.*, 1999; *Meeker and Mayewski*, 2002; *Brönnimann et al.*, 2007].

[17] The unprecedented long-lasting increase in atmospheric dust production after 1870 (Figure 3), can be explained by the recent human-induced land degradation in the Sahel [*Moulin and Chiapello*, 2006] or by the climate response to anthropogenic forcing leading to unusual positive phases of NAO during winter time [*Shindell et al.*, 2001]. However, the presence of high amounts of dust before that time as well as the comparison with instrumental climatic data rather supports the hypothesis of a dominant large-scale climatic control on the dust export also in the 19th and 20th century [*Moulin et al.*, 1997]. In fact, the second greatest dust deposition from our record that occurred in 1977 can precisely be correlated to the most severe drought ever recorded in Sudano-Sahelian zone (i.e., the driest year since records began in 1931 [*Middleton*, 1985]). Moreover, the very low meridional Saharan dust flux recorded around 1942 was synchronous with an extreme state of the global troposphere-stratosphere system in northern winter from 1940 to 1942, consistent with a weak polar vortex and a negative phase of the NAO [*Brönnimann et al.*, 2004; *Bakke et al.*, 2008].

4.2. Carbonaceous Aerosols From Biomass and Fossil Fuel Combustion

[18] The Colle Gnifetti BC record (Figure 3) revealed a major drop around 1570 that is synchronous with an increase in dust-laden winds from the Sahara and with Northern Hemisphere atmospheric circulation changes (see section 4.1). The carbon isotopic composition of BC ($\delta^{13}C_{BC}$), which provides information about the type of vegetation being burnt (i.e., reflecting C_3 and C_4 pathways of photosynthetic carbon assimilation [*Cachier et al.*, 1989; *Clark et al.*, 2001]) ranges between −23 and −26‰ over the last millennium, indicating that C_3 woody (−27‰) pyrogenic emissions were larger than C_4 grassland (−13‰) burning (C_3:C_4 ratio of burnt biomass is 75:25). This pattern of increased C_3 burning is particularly prominent between 1570 and 1750, when the pyrogenic emissions were the lowest (BC is 7 ± 2 μg BC kg^{-1}; C3:C4 ratio of burnt biomass is 90:10), therefore excluding a period of deforestation in Europe. Meanwhile, historic data [*Pfister*, 1984, 2005] showed that climatic anomalies and natural disasters involved recurrent socioeconomic crises between 1570 and 1630, when years "without summer" and severe winters were frequent in Europe. Moreover, proxy records and precipitation reconstructions indicate between approximately 1500–1800 wetter climatic conditions, likely caused by an increase in summer precipitation [*Casty et al.*, 2005; *Magny et al.*, 2008]. The abrupt drop in biomass burning activity and especially in C_4 grassland burning could therefore indicate reduced agricultural practices during this cold and wet period of the LIA [*Glaser*, 1995], most probably associated with stronger North Atlantic southwesterlies and an increase in spring/summer precipitation (see section 4.1).

[19] The Colle Gnifetti ice core showed high woody pyrogenic emissions between approximately 1000 and 1570 related to human activity, which contrasts to the subsequent decrease in grassland burning between 1570 and 1750. A decrease in grassland burning from 1500 to 1700 has been also reported from an Antarctic atmospheric record [*Ferretti et al.*, 2005]. Although this could suggest a global trend, the observation from the Swiss Alps of this time period strikingly coincides with the end of the "Walser" period, the last cultural tradition responsible for

extended settlement and important land use changes in the area: The Walser Alemanic people migrated from the Valais after 1200 and settled around the Monte Rosa Massif until 1500, when their numbers declined [*Pawson and Egli*, 2001; *Malacarne et al.*, 2005; *Maurer et al.*, 2006], documenting climatic deterioration and unfavorable environmental conditions. Furthermore, an important decrease in biomass burning activity was also registered north of the Alps between approximately 1500 and 1700 in charcoal sedimentary records from Lake Lucerne and Lake Joux (Switzerland), supporting the hypothesis for a regional decrease in biomass burning activity indirectly triggered by climatic-driven environmental changes [*Thevenon and Anselmetti*, 2007; *Magny et al.*, 2008].

[20] After 1750, $\delta^{13}C_{BC}$ values abruptly shift from values lower than −25‰ to values higher than −24‰, therefore strongly suggesting a major change in type of combustible (e.g., fossil wood/charcoal) that occurred one century before the European Industrial Revolution of approximately 1850, but synchronously with the beginning of the fossil fuel era [*Andres et al.*, 1999]. The average BC values increase from 7 μg kg^{-1} for the time period from 1750 to 1850, to 13 μg kg^{-1} from 1850 to 1950, and to 20 μg kg^{-1} from 1950 to 1980. A peculiar BC peak is observed between 1875 and 1885 (Figure 3), i.e., just after the beginning of the Industrial Revolution, and synchronously with the gradual increase of massive coal emissions, which overtook those from biofuel after 1880 [*Bond et al.*, 2007]. Afterward, the BC emissions to the atmosphere rise exponentially (Figure 3), although a moderate local impact cannot be definitively ruled out, because this time period coincides with the beginning of the tourism in the area and the building of mountain refuges (e.g., Capanna Gnifetti in 1876, 3647 m asl; Capanna Monte Rosa in 1885, 2795 m asl; and Capanna Margherita in 1893, 4454 m asl) as well as the opening of the Gornergrat electric railway in 1898 (approximately 9 km from the coring site, terminal station at 3089 m asl).

[21] Although fossil fuels have on average the same $\delta^{13}C$ as wood, the decreasing trend observed in the $\delta^{13}C_{BC}$ data (from approximately −24 to −25‰) over the two last centuries in the Colle Gnifetti record could reflect the increasing contribution from fossil fuel emissions [*Reddy et al.*, 2002; *Jenk et al.*, 2006]. This hypothesis is supported by the recent lowest $\delta^{13}C_{BC}$ values coinciding with BC peaks, while the two latest highest $\delta^{13}C_{BC}$ values around 1915 and 1940, respectively, coincide with the First and Second World War and reduced smelter emissions (Figure 3). Finally, some well-preserved organic and vegetation remains (fungi spores, pollen, green algae, and charcoal/wood particles) were also frequently found in the ice (Figure 5), pointing out the long-range transport of relatively large microorganisms to high altitudes. Large charcoal particles (>30 μm) were found throughout the core, whereas organic and inorganic fly ash particles were detected after approximately 1790, documenting the long-range atmospheric transport of fossil fuel particulate emissions from that time and, in particular, during modern times (1950–1980).

5. Conclusions

[22] The developments of optical and chemical approaches for studying natural and anthropogenic primary aerosols successfully characterize the lithogenic and combustion aerosols, respectively. This study also stresses the necessity to calibrate under interlaboratory reproducible analytical conditions the methods with microgram-level quantity of standards that can reflect the behavior of nonhomogeneous aerosols.

[23] The Colle Gnifetti summer ice archive analysis demonstrates that the BC aerosol record is independent of the large-scale climatic control affecting the transport of mineral dust to the Southern Alps, but primarily reflects regional-scale anthropogenic activity. The $\delta^{13}C$ composition of the BC emissions indicates that wood contributed to the largest fraction of preindustrial BC emissions (7 μg C kg^{-1}), especially when a major drop in biomass burning activity occurred between 1570 and 1750, probably in association with decreased agricultural practices triggered by wetter summer climatic conditions during this part of the LIA. Another shift in the $\delta^{13}C_{BC}$ emissions occurred around 1750, synchronously with the beginning of the fossil fuel era. Afterward, BC increased subsequently to 13 μg C kg^{-1} in the transition era (1850–1950) and to 20 μg C kg^{-1} in modern times (1950–1980).

[24] Unlike the BC deposition, the mineral dust transport to the summits of the Southern Alps is primarily controlled by large-scale climatic patterns (i.e., drier winter in North Africa and stronger southwesterlies over the North Atlantic), leading to transport of massive dust plumes from the Sahara around 1200–1300, 1430–1520, 1570–1690, 1780–1800, and after 1870. In contrast, the periods of low Saharan dust deposition in between those periods (around 1000–1200, 1520–1570, 1690–1780 and 1800–1870) may indicate weaker meridional atmospheric circulation at that times, leading to colder and drier spring/summer conditions over Western and Central Europe. Beside the recent anthropogenic climate forcing, our results suggest that such atmospheric features were probably influenced by coupled ocean-atmosphere patterns, primarily forced by changes in solar irradiance rather than by explosive volcanism activity. Moreover the unprecedented strong Saharan dust event that occurred in the late eighteen century coincided with low-latitude atmospheric changes, providing a useful analog for a better understanding of large-scale atmospheric teleconnection patterns. Eventually, these time series on the black carbonaceous and iron-containing dust particles that were emitted to the atmosphere over the last millennium will help to better apprehend the direct (incident solar radiation) and indirect climate forcings (e.g., effect of dust and BC on clouds and snow albedo, or uptake of atmospheric carbon dioxide by marine microorganisms) of the primary aerosol emissions on past European climate.

[25] **Acknowledgments.** We are grateful to the Colle Gnifetti consortium and to the drilling team, Paolo Gabrielli, Frederic Planchon, Beat Rufibach, Aurel Schwerzmann, Margit Schwikowski, and Dieter Stampfli, for the recovery of the ice core. We wish to thank W. Halter and M. Guillong for conducting LA-ICP-MS analyses. We acknowledge F. Giraud for allowing the use of the automated transmitted microscope from the micropaleontology laboratory of the ETH of Zurich and M. Coray Strasser, S. Köchli, S. Brütsch, and M. Sigl for laboratory assistance. We thank, in particular, H. Cachier and S. Szidat for fruitful scientific exchanges, T. M. Jenk for giving access to the age model, and anonymous reviewers for their constructive comments and suggestions. This work was supported by the French Ministry of Foreign Affairs (Lavoisier postdoctoral fellowship), the Swiss National Science Foundation (SNF, Ambizione fellowship), the NCCR Climate program of the SNF (projects VITA and VIVALDI), the EU FP6 project MILLENNIUM

(017008), and the Istituto Nazionale per la Ricerca Scientifica e Tecnologica sulla Montagna (INRM), and received additional support from the ETH of Zurich and the University of Bern.

References

Adedokun, J. A., W. O. Emofurieta, and O. A. Adedeji (1989), Physical, mineralogical and chemical properties of Harmattan dust at Ile-Ife, Nigeria, *Theor. Appl. Climatol.*, *40*, 161–169, doi:10.1007/BF00866179.

Alean, J., W. Haeberli, and B. Schädler (1983), Snow accumulation, firn temperature and solar radiation in the area of the Colle Gnifetti core drilling site (Monte Rosa, Swiss Alps): Distribution patterns and interrelationships, *Z. Gletscherkd. Glazialgeol.*, *19*(2), 131–147.

Andres, R. J., D. J. Fielding, G. Marland, T. A. Boden, and N. Kumar (1999), Carbon dioxide emissions from fossil-fuel use, 1751–1950, *Tellus Ser. B*, *51*, 759–765.

Bakke, J., Ø. Lie, S. O. Dahl, A. Nesje, and A. E. Bjune (2008), Strength and spatial patterns of the Holocene wintertime westerlies in the NE Atlantic region, *Global Planet. Change*, *60*, 28–41, doi:10.1016/j.gloplacha.2006.07.030.

Black, D. E., L. C. Peterson, J. T. Overpeck, A. Kaplan, M. N. Evans, and M. Kashgarian (1999), Eight centuries of North Atlantic Ocean atmosphere variability, *Science*, *286*, 1709–1713, doi:10.1126/science.286.5445.1709.

Bond, T. C., E. Bhardwaj, R. Dong, R. Jogani, S. Jung, C. Roden, D. G. Streets, and N. M. Trautmann (2007), Historical emissions of black and organic carbon aerosol from energy-related combustion, 1850–2000, *Global Biogeochem. Cycles*, *21*, GB2018, doi:10.1029/2006GB002840.

Brönnimann, S., J. Luterbacher, J. Staehelin, and T. M. Svendby (2004), An extreme anomaly in stratospheric ozone over Europe in 1940–1942, *Geophys. Res. Lett.*, *31*, L08101, doi:10.1029/2004GL019611.

Brönnimann, S., E. Xoplaki, J. Luterbacher, C. Casty, and A. Pauling (2007), ENSO influence on Europe during the last centuries, *Clim. Dyn.*, *28*, 181–197, doi:10.1007/s00382-006-0175-z.

Cachier, H., M. P. Bremond, and P. Buat-Menard (1989), Carbonaceous aerosols from different tropical biomass burning sources, *Nature*, *340*, 371–373, doi:10.1038/340371a0.

Casty, C., H. Wanner, J. Luterbacher, J. Esper, and R. Böhm (2005), Temperature and precipitation variability in the European Alps since 1500, *Int. J. Climatol.*, *25*, 1855–1880, doi:10.1002/joc.1216.

Charles, C. D., D. E. Hunter, and R. G. Fairbanks (1997), Interaction between the ENSO and the Asian monsoon in a coral record of tropical climate, *Science*, *277*, 925–928, doi:10.1126/science.277.5328.925.

Chiapello, I., and C. Moulin (2002), TOMS and METEOSAT satellite records of the variability of Saharan dust transport over the Atlantic during the last two decades (1979–1997), *Geophys. Res. Lett.*, *29*(8), 1176, doi:10.1029/2001GL013767.

Chylek, P., B. Johnson, P. A. Damiano, K. C. Taylor, and P. Clement (1995), Biomass burning record and black carbon in the GISP2 ice core, *Geophys. Res. Lett.*, *22*(2), 89–92, doi:10.1029/94GL02841.

Clark, J. S., E. C. Grimm, J. Lynch, and P. J. Mueller (2001), Effects of Holocene climate change on the C4 grassland/woodland boundary in the northern Central Plains, *Ecology*, *82*, 620–636.

Cole, J. E., R. B. Dunbar, T. R. McClanahan, and N. A. Muthiga (2000), Tropical Pacific forcing of decadal SST variability in the western Indian Ocean over the past two centuries, *Science*, *287*(5453), 617–619, doi:10.1126/science.287.5453.617.

Collaud Coen, M., E. Weingartner, D. Schaub, C. Hueglin, C. Corrigan, S. Henning, M. Schwikowski, and U. Baltensperger (2004), Saharan dust events at the Jungfraujoch: Detection by wavelength dependence of the single scattering albedo and first climatology analysis, *Atmos. Chem. Phys.*, *4*, 2465–2480.

Crowley, T. J. (2000), Causes of climate change over the past 1000 years, *Science*, *289*, 270–277, doi:10.1126/science.289.5477.270.

Dawson, A. G., K. Hickey, P. A. Mayewski, and A. Nesje (2007), Greenland (GISP2) ice core and historical indicators of complex North Atlantic climate changes during the fourteenth century, *Holocene*, *17*, 427–434, doi:10.1177/0959683607077010.

Delmonte, B., I. Basile-Doelsch, J. R. Petit, V. Maggi, M. Revel-Rolland, A. Michard, E. Jagoutz, and F. Grousset (2004), Comparing the EPICA and Vostok dust records during the last 220,000 years: Stratigraphical correlation and provenance in glacial periods, *Earth Sci. Rev.*, *66*, 63–87, doi:10.1016/j.earscirev.2003.10.004.

Döscher, A., H. W. Gäggeler, U. Schotterer, and M. Schwikowski (1995), A 130 years deposition record of sulphate, nitrate, and chloride from a high-Alpine glacier, *Water Air Soil Pollut.*, *85*, 603–609, doi:10.1007/BF00476895.

Eichler, A., M. Schwikowski, M. Furger, U. Schotterer, and H. W. Gäggeler (2004), Sources and distribution of trace species in Alpine precipitation inferred from two 60-year ice core paleorecords, *Atmos. Chem. Phys. Discuss.*, *4*, 71–108.

Ferretti, D. F., et al. (2005), Unexpected changes to the global methane budget over the past 2000 years, *Science*, *309*, 1714–1717, doi:10.1126/science.1115193.

Glaser, R. (1995), T hermische klimaentwicklung in Mitteleuropa seit dem jahr 1000, *Geowissenschaften*, *13*, 302–312.

Goudie, A. S., and N. J. Middleton (2001), Saharan dust storms: Nature and consequences, *Earth Sci. Rev.*, *56*(1–4), 179–204, doi:10.1016/S0012-8252(01)00067-8.

Grove, J. (1987), *The Little Ice Age*, 498 pp., Methuen, London.

Haeberli, W., and M. Funk (1991), Borehole temperatures at the Colle Gnifetti core drilling site (Monte Rosa, Swiss Alps), *J. Glaciol.*, *37*(125), 37–46.

Haeberli, W., U. Schotterer, D. Wagenbach, H. Haeberli-Schwitter, and S. Bortenschlager (1983), Accumulation characteristics on a cold, high-Alpine firn saddle from a snow-pit study on Colle Gnifetti, Monte Rosa, Swiss Alps, *J. Glaciol.*, *29*(102), 260–271.

Highwood, E.-J., and D. S. Stevenson (2003), Atmospheric impact of the 1783–1784 Laki eruption: Part II. Climatic effect of sulphate aerosol, *Atmos. Chem. Phys.*, *3*, 1177–1189.

Intergovernmental Panel on Climate Change (IPCC) (2007), Summary for policymakers, in *Climate Change 2007: The Physical Science Basis: Contribution of Working Group I to the Fourth Assessment Report of the Intergovernmental Panel on Climate Change*, edited by S. Solomon et al., chap. 6, pp. 434–497, Cambridge Univ. Press, Cambridge, U. K.

Jenk, T. M., S. Szidat, M. Schwikowski, H. W. Gäggeler, S. Brütsch, L. Wacker, , H.-A. Synal, and M. Saurer (2006), Radiocarbon analysis in an Alpine ice core: Record of anthropogenic and biogenic contributions to carbonaceous aerosols in the past (1650–1940), *Atmos. Chem. Phys.*, *6*, 5381–5390.

Jenk, T. M., S. Szidat, D. Bolius, M. Sigl, H. W. Gaggeler, L. Wacker, M. Ruff, C. Barbante, C. F. Boutron, and M. Schwikowski (2009), A novel radiocarbon dating technique applied to an ice core from the Alpsindicates late Pleistocene ages, *J. Geophys. Res.*, *114*, D14305, doi:10.1029/2009JD011860.

Jones, P. D., T. J. Osborn, and K. R. Briffa (2003), Pressure-based measures of the North Atlantic Oscillation (NAO): A Comparison and an assessment of changes in the strength of the NAO and in its influence on surface climate parameters, in *The North Atlantic Oscillation: Climatic Significance and Environmental Impact*, *Geophys. Monogr. Ser.*, vol. 134, edited by J. W. Hurrell et al., pp. 51–62, AGU, Washington, D. C.

Krueger, B. J., V. H. Grassian, J. P. Cowin, and A. Laskin (2004), Heterogeneous chemistry of individual mineral dust particles from different dust source regions: The importance of particle mineralogy, *Atmos. Environ.*, *38*, 6253–6261, doi:10.1016/j.atmosenv.2004.07.010.

Lavanchy, V. M. H., H. W. Gäggeler, U. Schotterer, M. Schwikowski, and U. Baltensperger (1999), Historical record of carbonaceous particle concentrations from a European high-Alpine glacier (Colle Gnifetti, Switzerland), *J. Geophys. Res.*, *104*, 21,227–21,236, doi:10.1029/1999JD900408.

Lean, J., and D. Rind (1999), Evaluating sun-climate relationships since the Little Ice Age, *J. Atmos. Sol. Terr. Phys.*, *61*, 25–36, doi:10.1016/S1364-6826(98)00113-8.

Luterbacher, J., et al. (2002), Extending North Atlantic Oscillation reconstructions back to 1500, *Atmos. Sci. Lett.*, *2*, 114–124, doi:10.1006/asle.2001.0044.

Lüthi, M., and M. Funk (2000), Dating ice cores from a high Alpine glacier with a flow model for cold firn, *Ann. Glaciol.*, *31*, 69–79, doi:10.3189/172756400781820381.

Magny, M., E. Gauthier, B. Vannière, and O. Peyron (2008), Palaeohydrological changes and human-impact history over the last millennium recorded at Lake Joux in the Jura Mountains, Switzerland, *Holocene*, *18*(2), 255–265, doi:10.1177/0959683607086763.

Malacarne, E., M. E. Danubio, and G. Gruppioni (2005), The effects of geographical and prolonged cultural isolation on the marital behaviour of an Alpine community (Valsesia-Italy, 1618–1899), *Hum. Evol.*, *20*(2–3), 167–179, doi:10.1007/BF02438734.

Mann, M. E. (2007), Climate over the past two millennia, *Annu. Rev. Earth Planet. Sci.*, *35*, 111–136, doi:10.1146/annurev.earth.35.031306.140042.

Maupetit, F., D. Wagenbach, P. Weddeling, and R. J. Delmas (1995), Seasonal fluxes of major ions to a high altitude cold Alpine glacier, *Atmos. Environ.*, *29*(1), 1–9, doi:10.1016/1352-2310(94)00222-7.

Maurer, K., A. Weyand, M. Fischer, and J. Stöcklin (2006), Old cultural traditions, in addition to land use and topography, are shaping plant diversity of grasslands in the Alps, *Biol. Conserv.*, *130*, 438–446, doi:10.1016/j.biocon.2006.01.005.

Meeker, L. D., and P. A. Mayewski (2002), A 1400 year long record of atmospheric circulation over the North Atlantic and Asia, *Holocene*, *12*(3), 257–266, doi:10.1191/0959683602hl542ft.

Metrich, N., H. Sigurdsonn, P. S. Meyer, and J. D. Devine (1991), The 1783 Lakagigar eruption in Iceland: Geochemistry, CO^2 and sulfur degassing, *Contrib. Mineral. Petrol.*, *107*, 435–447, doi:10.1007/BF00310678.

Middleton, N. J. (1985), Effect of drought on dust production in the Sahel, *Nature*, *316*, 431–434, doi:10.1038/316431a0.

Moreno, T., X. Querol, S. Castillo, A. Alastuey, E. Cuevas, L. Herrmann, M. Mounkaila, J. Elvira, and W. Gibbons (2006), Geochemical variations in aeolian mineral particles from the Sahara-Sahel dust corridor, *Chemosphere*, *65*(2), 261–270, doi:10.1016/j.chemosphere.2006.02.052.

Moulin, C., and I. Chiapello (2006), Impact of human-induced desertification on the intensification of Sahel dust emission and export over the last decades, *Geophys. Res. Lett.*, *33*, L18808, doi:10.1029/2006GL025923.

Moulin, C., C. E. Lambert, F. Dulac, and U. Dayan (1997), Control of atmospheric export of dust from North Africa by the North Atlantic Oscillation, *Nature*, *387*(6634), 691–694, doi:10.1038/42679.

Oeschger, H., U. Schotterer, B. Stauffer, W. Haeberli, and H. Röthlisberger (1977), First results from Alpine core drilling projects, *Z. Gletscherkd. Glazialgeol.*, *13*, 193–208.

Pawson, E., and H.-R. Egli (2001), History and discovery of the European and New Zealand Alps, *Mt. Res. Dev.*, *21*(4), 350–358, doi:10.1659/0276-4741(2001)021[0350:HARDOT]2.0.CO;2.

Pfister, C. (1984), *Das Klima der Schweiz 1525–1860: Das Klima der Schweiz und Seine Bedeutung in der Geschichte von Bevölkerung und Landwirtschaft*, Paul Haupt, Bern.

Pfister, C. (2005), Weeping in the snow—The second period of Little Ice Age-type crises, 1570 to 1630, in *Cultural Consequences of the Little Ice Age*, edited by W. Behringer, H. Lehmann, and C. Pfister, pp. 31–85, Vandenhoeck & Ruprecht, Göttingen, Germany.

Prospero, J. M., and R. T. Nees (1986), Impact of the North African drought and El Niño on mineral dust in the Barbados trade winds, *Nature*, *320*, 735–738, doi:10.1038/320735a0.

Reddy, C. M., A. Pearson, L. Xu, A. P. McNichol, B. A. Benner Jr., S. A. Wise, G. A. Klouda, L. A. Currie, and T. I. Eglinton (2002), Radiocarbon as a tool to apportion the sources of polycyclic aromatic hydrocarbons and black carbon in environmental samples, *Environ. Sci. Technol.*, *36*, 1774–1782, doi:10.1021/es011343f.

Ruth, U., D. Wagenbach, J. P. Steffensen, and M. Bigler (2003), Continuous record of microparticle concentration and size distribution in the central Greenland NGRIP ice core during the lastglacial period, *J. Geophys. Res.*, *108*(D3), 4098, doi:10.1029/2002JD002376.

Schmutz, C., J. Luterbacher, D. Gyalistras, E. Xoplaki, and H. Wanner (2000), Can we trust proxy-based NAO index reconstructions?, *Geophys. Res. Lett.*, *27*, 1135–1138, doi:10.1029/1999GL011045.

Schotterer, U., H. Oeschger, D. Wagenbach, and K. Munnich (1985), Information on paleo-precipitation on a high-altitude glacier Monte Rosa, Switzerland, *Z. Gletscherkd. Glazialgeol.*, *21*(85), 379–388.

Schwikowski, M., P. Seibert, U. Baltensperger, and H. W. Gäggeler (1995), A study of an outstanding Saharan dust event at the high-Alpine Site Jungfraujoch, Switzerland, *Atmos. Environ.*, *29*(15), 1829–1842, doi:10.1016/1352-2310(95)00060-C.

Shindell, D. T., G. A. Schmidt, M. E. Mann, D. Rind, and A. Waple (2001), Solar forcing of regional climate change during the Maunder Minimum, *Science*, *294*, 2149–2152, doi:10.1126/science.1064363.

Sodemann, H., A. S. Palmer, C. Schwierz, M. Schwikowski, and H. Wernli (2006), The transport history of two Saharan dust events archived in an Alpine ice core, *Atmos. Chem. Phys.*, *6*, 667–688.

Thevenon, F., and F. Anselmetti (2007), Charcoal and fly ash particles from Lake Lucerne sediments (Central Switzerland) characterized by image analysis: Anthropologic, stratigraphic and environmental implications, *Quat. Sci. Rev.*, *26*, 2631–2643, doi:10.1016/j.quascirev.2007.05.007.

Thevenon, F., D. Williamson, A. Vincens, M. Taieb, O. Merdaci, M. Decobert, and G. Buchet (2003), A Late Holocene charcoal record from Lake Masoko, SW Tanzania: Climatic and anthropologic implications, *Holocene*, *13*(5), 785–792, doi:10.1191/0959683603hl665rr.

Thevenon, F., E. Bard, D. Williamson, and L. Beaufort (2004), A biomass burning record from the west equatorial Pacific over the last 360 kyr: Methodological, climatic and anthropic implications, *Palaeogeogr. Palaeoclimatol. Palaeoecol.*, *213*, 83–99.

Thompson, L. G., T. Yao, E. Mosley-Thompson, M. E. Davis, K. A. Henderson, and P.-N. Lin (2000), A high-resolution millennial record of the South Asian monsoon from Himalayan ice cores, *Science*, *289*, 1916–1919, doi:10.1126/science.289.5486.1916.

Wagenbach, D., and K. Geis (1989), The mineral dust record in a high-altitude Alpine glacier (Colle Gnifetti, Swiss Alps), in *Paleoclimatology and Paleometeorology: Modern and Past Patterns of Global Atmospheric Transport*, *NATO Adv. Sci. Inst. Ser. C*, vol. 282, edited by M. Leinen and M. Sarnthein, pp. 543–564, Kluwer Acad., Dordrecht, Netherlands.

Wagenbach, D., U. Görlach, K. Haffa, H. G. Junghans, K. O. Münnich, and U. Schotterer (1985), A long-term aerosol deposition record in a high-altitude Alpine glacier, *World Meteorol. Organ. Rep. 647*, pp. 623–631, World Meteorol. Organ., Geneva, Switzerland.

F. S. Anselmetti, Eawag, Swiss Federal Institute of Aquatic Science and Technology, Überlandstrasse 133, P.O. Box 611, CH-8600 Dübendorf, Switzerland.

S. M. Bernasconi, Geological Institute, ETH Zurich, NO G 53.3, Sonneggstrasse 5, CH-8092 Zurich, Switzerland.

M. Schwikowski, Paul Scherrer Institut, OFLB 109, 5232 Villigen, CH-5232 Villigen, Switzerland.

F. Thevenon, F.-A. Forel Institute, University of Geneva, 10 Route de Suisse, CH-1290 Versoix, Switzerland. (florian.thevenon@yahoo.fr)